Eur. Phys. J. D **9**, 217–221 (1999)

THE EUROPEAN PHYSICAL JOURNAL D

EDP Sciences

Many-body effects and autoionization resonances in the photoionization of simple metal clusters

M.E. Madjet and P.A. Hervieux

L.P.M.C, Institut de Physique, Technopôle 2000, F-57078 Metz, France

Received: 2 September 1998 / Received in final form: 15 December 1998

Abstract. Within the framework of the time-dependent local-density approximation (TDLDA) and the spherical background jellium model, we have estimated the photoionization cross sections for a medium-size closed-shell sodium cluster, Na_{20}. We have also introduced a self-interaction correction to ensure the correct asymptotic behaviour of the potential seen by the ejected electron. Our results show that in contrast to the photoexcitation process, the photoionization cross sections are very sensitive to the approximation used to describe the cluster electrons. Futhermore, many-electron correlations are found to be very large. Similarly to the atomic case, when correct asymptotic conditions are taken properly into account, cross sections exhibit many one-electron autoionization resonances.

PACS. 36.40.Gk Plasma and collective effects in clusters – 32.80.Dz Autoionization

1 Introduction

If the photon energy of an excited quantum system exceeds the binding energy, photoelectron emission can occur. In contrast with the the photoexcitation process of simple metal clusters, which has been extensively studied in the past, only a few theoretical works have been devoted to the study of the photoionization process [1–3]. The existence of many *active* electrons in the cluster implies that one must use a truly many-electron theory. Thus, from the theoretical point of view, this process is of fundamental interest, since it provides a very powerful tool for studying many-electron correlations in finite quantum systems.

We know from atomic physics that one can never reach a good agreement between theoretical predictions and experimental results for photoionization cross sections if electronic correlation effects are not taken into account in the theoretical models (e.g., RPA, MBPT, and TDLDA). Under the condition that the external field is weak, the simplest way to implement such a theory is to work in the framework of the time-dependent local-density approximation (TDLDA). This latter approximation has been used with success for the first time by Zangwill and Soven [4] for the study of photoionization in rare gases. Futhermore, this formalism has been also successfully extended to the study of photoinization of molecules [5]. Recently, in the context of atomic physics and density functional theory, Stener *et al.* [6] have shown the importance of using exchange-correlation potentials with correct asymptotic behaviour. In fact, since these potentials are able to support virtual Rydberg states, it allows one to consider one-electron excitation resonances (Feshbach resonances, autoionization resonances) during photoionization. The shape of these resonances are characterized by the so-called Fano profile [7]. The aim of the present work is to find answers to the following questions: What is the importance of the many-electron correlations in the photoinization process when alkali-metal clusters are investigated? Do the photoinization cross sections exhibit autoionization resonances when correct asymptotic conditions and an N-body theory are used? Our goal is also to provide quantitative photoionization cross sections in order to stimulate future experiments.

Closed-shell simple metal clusters are usually well described by the spherical jellium model [8], which consists in the replacement of the real ionic core potential by a constant positive background. Within this model and the TDLDA method, we have estimated photoionization cross sections for a medium-size closed-shell sodium cluster, Na_{20}. In order to ensure the correct asymptotic behaviour of the potential seen by the ejected electron, a self-interaction correction (SIC) has also been introduced. Our theoretical approach is briefly outlined in the next section. Results concerning the closed-shell neutral cluster Na_{20} as well as a conclusion are given in Sect. 3. Atomic units are used unless otherwise specified.

2 Theoretical method

2.1 Cluster description

The cluster is described in the spherical background jellium model. This model consists in the replacement of the real ionic core potential by a constant positive background

corresponding to a uniformly distributed charge density. For a metal cluster having A singly charged ionic cores, this potential is given by

$$V_{\rm jel}(r) = \begin{cases} -\frac{A}{2R_{\rm C}}\left[3-\left(\frac{r}{R_{\rm C}}\right)^2\right] & \text{for } r \le R_{\rm C} \\ -\frac{A}{r} & \text{for } r > R_{\rm C} \end{cases} , \quad (1)$$

where $R_{\rm C} = A^{1/3} r_s$ and r_s is the Wigner–Seitz radius. In the Kohn–Sham formulation of density functional theory, the ground-state electronic density $\varrho_{\rm C}$ of an N-electron system is written in terms of single-particle orbitals ϕ_i:

$$\varrho_{\rm C}(\mathbf{r}) = \sum_{i=1}^{N} \varrho_i(\mathbf{r}) = \sum_i |\phi_i(\mathbf{r})|^2 . \quad (2)$$

These orbitals obey the Schrödinger equation

$$\left[-\frac{1}{2}\nabla^2 + V_{\rm KS}(\mathbf{r})\right]\phi_i(\mathbf{r}) = \epsilon_i \phi_i(\mathbf{r}) , \quad (3)$$

where $V_{\rm KS}(\mathbf{r})$ is an effective single-particle potential given by

$$V_{\rm KS}(\mathbf{r}) = V_{\rm jel}(\mathbf{r}) + V_{\rm H}(\varrho_{\rm C}(\mathbf{r})) + V_{\rm xc}(\varrho_{\rm C}(\mathbf{r})) , \quad (4)$$

where $V_{\rm H}(\varrho_{\rm C}(\mathbf{r}))$ is the Hartree potential and $V_{\rm xc}(\varrho_{\rm C}(\mathbf{r}))$ the exchange-correlation potential. Since the form of $V_{\rm xc}$ is not known in general, several approximations have been proposed in the literature. In this work, we have used the form obtained by Gunnarsson and Lundqvist [9] in the framework of the local-density approximation (LDA):

$$V_{\rm xc}(\varrho_{\rm C}(\mathbf{r})) = -\left(\frac{3\varrho_{\rm C}(\mathbf{r})}{\pi}\right)^{1/3} - 0.0333 \log\left(1+\frac{11.4}{r_s(\mathbf{r})}\right) \quad (5)$$

where $r_s(\mathbf{r}) = [3/4\pi\varrho_{\rm C}(\mathbf{r})]^{1/3}$ is the local Wigner–Seitz radius. For a neutral cluster, the asymptotic behaviour of $V_{\rm KS}$ is given by the exchange contribution to $V_{\rm xc}$, which behaves at large distance as $\varrho_{\rm C}(\mathbf{r})^{1/3}$. As a consequence, the Kohn–Sham potential $V_{\rm KS}$ decreases exponentially to zero, i.e., it does not reproduce the correct $1/r$ asymptotic behaviour. This problem does not appear in the Hartree–Fock (HF) theory, because the HF exchange potential exactly compensates the self-interaction term contained in the Hartree potential. Following Perdew and Zunger [14], we have added a self-interaction correction (SIC) that restores the correct asymptotic behaviour of the potential (we will call this method LDA-SIC). This procedure has been succesfully applied to the study of both ground- and excited-state properties of small metal clusters [10–13]. The corrected Kohn–Sham potential $V^i_{\rm SIC}$ is then given by

$$V^i_{\rm SIC}(\mathbf{r}) = V_{\rm jel}(\mathbf{r}) + \int \frac{[\varrho_{\rm C}(\mathbf{r}') - \varrho_i(\mathbf{r}')]{\rm d}\mathbf{r}'}{|\mathbf{r}-\mathbf{r}'|} + V_{\rm xc}[\varrho_{\rm C}(\mathbf{r})] - V_{\rm xc}[\varrho_i(\mathbf{r})] , \quad (6)$$

where ϱ_i is the i single-particle density defined in (2). It is easy to check that, as in HF theory, the resulting potential has the correct $-1/r$ behaviour at large distances.

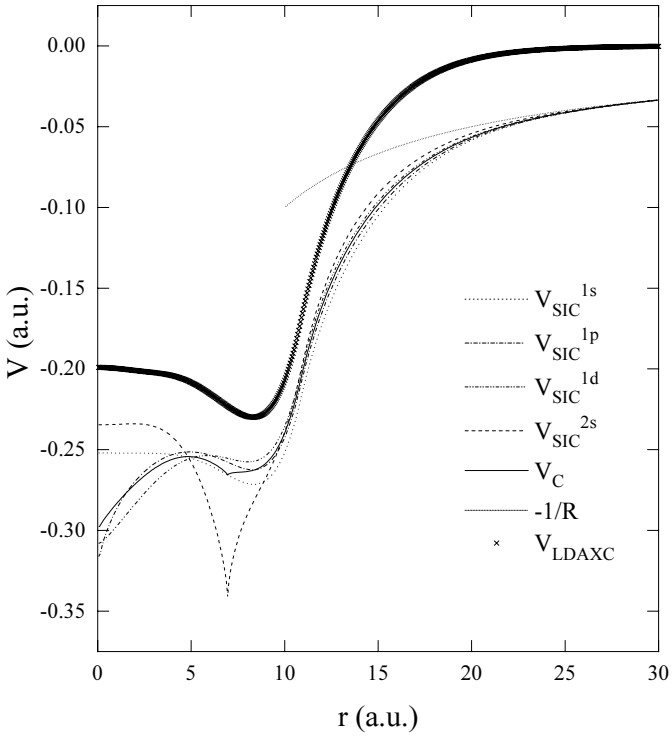

Fig. 1. Comparison between the $V^i_{\rm sic}$ potentials and the LDA one for Na_{20}. The function $\frac{-1}{R}$ is also shown, broken curve.

Table 1. Ionization potential (in eV) of the occupied single-particle states of Na_{20} calculated in the approximations LDA and LDA-SIC.

Orbital	LDA	LDA-SIC
$1s$	5.109	6.340
$1p$	4.393	5.415
$1d$	3.440	4.327
$2s$	2.810	3.837

Notice also that the $V^i_{\rm SIC}$ potential is now explicitly state-dependent. It should be noted that, because the potential is orbital dependent, the various ground-state orbitals are no longer orthogonal. However, the work of Perdew and Zunger [14] indicates that the degree of nonothogonality is very small. Consequently, we do not minimize the LDA-SIC functional under the orthogonality constraint, and we assume that this will not change appreciably the presented results. Figure 1 shows a comparison between the original LDA potential and the calculated $V^i_{\rm SIC}$ potentials for the occupied orbitals $1s$, $1p$, $1d$, and $2s$ of Na_{20}. The corresponding ionization potentials are given in Table 1.

2.2 Time-dependent local-density approximation and photoionization cross section

If the system is in a weak external field of frequency ω, the theory of the linear response relates the induced electronic

density $\delta\varrho(\mathbf{r};\omega)$ to the external potential $V_{\rm ext}(\mathbf{r};\omega)$ by the relation

$$\delta\varrho(\mathbf{r};\omega) = \int \chi(\mathbf{r},\mathbf{r}';\omega)\, V_{\rm ext}(\mathbf{r}';\omega)\, \mathrm{d}\mathbf{r}', \tag{7}$$

where $\chi(\mathbf{r},\mathbf{r}';\omega)$ is the dynamic response function. For the photoionization process, $V_{\rm ext}(\mathbf{r};\omega)$ takes the form

$$V_{\rm ext}(\mathbf{r};\omega) = \sum_{j=1}^{N_{\rm e}} \sqrt{\frac{4\pi}{3}}\, \mathcal{V}_{\rm ext}(r_j)\, Y_{10}(\hat{r}_j) = \sum_{j=1}^{N_{\rm e}} z_j, \tag{8}$$

where $N_{\rm e}$ is the number of electrons in the cluster, and $\mathcal{V}_{\rm ext}(r) = r$ is the radial part of $V_{\rm ext}$.

One defines also the self-consistent field $V_{\rm SCF}(\mathbf{r};\omega)$ as

$$V_{\rm SCF}(\mathbf{r};\omega) = V_{\rm ext}(\mathbf{r};\omega) + V_{\rm ind}(\mathbf{r};\omega), \tag{9}$$

where $V_{\rm ind}(\mathbf{r};\omega)$ is the induced field given by

$$V_{\rm ind}(\mathbf{r};\omega) = \int \frac{\delta\varrho(\mathbf{r};\omega)}{|\mathbf{r}-\mathbf{r}'|}\, \mathrm{d}\mathbf{r}' + \left[\frac{\partial V_{\rm xc}}{\partial\varrho}\right]_{\varrho=\varrho_{\rm C}} \delta\varrho(\mathbf{r};\omega). \tag{10}$$

The SCF potential has a spatial dependence of $V_{\rm SCF}(\mathbf{r};\omega) = \mathcal{V}_{\rm SCF}(r;\omega)P_1(\cos\theta)$. All the theoretical and technical details concerning the TDLDA applied to the photoionization process can be found in [1, 4].

In the dipole approximation, the independent-particle (LDA and LDA-SIC) photoionization cross section from an nl initial closed-subshell state to a $\epsilon l'$ final continuum state is given by the usual expression

$$\sigma_{nl}(\omega) = \frac{4\pi^2\omega}{3c}\frac{N_{nl}}{(2l+1)} \sum_{l'=l\pm1} \left|d_{nl,\epsilon l'}\right|^2, \tag{11}$$

with

$$d_{nl,\epsilon l'} = \sqrt{(2l+1)(2l'+1)} \begin{pmatrix} l & 1 & l' \\ 0 & 0 & 0 \end{pmatrix} \times \int_0^\infty P_{nl}(r)\mathcal{V}_{\rm ext}(r)P_{\epsilon l'}(r), \tag{12}$$

and where N_{nl} is the number of electrons in the nl subshell. As usual, the bound-state wave function is expanded as $\phi_i(\mathbf{r}) = \frac{P_{nl}(r)}{r}Y_{lm}(\hat{r})$ and the continuum wave function $P_{\epsilon l}$ behaves asymptotically as

$$P_{\epsilon l}(r) \overset{r\to\infty}{\sim} [\cos(\delta_l)F_l(kr) + \sin(\delta_l)G_l(kr)] = \sin\left(kr - \frac{1}{2}\pi + \frac{z}{k}\ln(2kr) + \Delta_l\right), \tag{13}$$

where the functions $F_l(kr)$ and $G_l(kr)$ are the regular and irregular spherical Coulomb functions respectively associated to the asymptotic charge z seen by the ejected electron and $\Delta_l = \sigma_l + \delta_l$, with the Coulomb phase shift $\sigma_l = \arg\Gamma(l+1-i\frac{z}{k})$. The total photoionization cross section is obtained from σ_{nl} by summation over all the initial states

$$\sigma(\omega) = \sum_{nl} \sigma_{nl}. \tag{14}$$

The difference between LDA and TDLDA comes from the difference between using the external potential of $V_{\rm ext}$ and that of $V_{\rm SCF}$. The self-consistent potential includes the phenomenon of screening. The time-dependent electric field coming from the photon is screened by the valence electrons of the metal cluster and, as we will see in the next section, this screening is important and is frequency-dependent. Thus, when many-electron correlations are included, the TDLDA partial photoionization cross section is calculated from (11) and (12) using $\mathcal{V}_{\rm SCF}(r;\omega)$ instead of $\mathcal{V}_{\rm ext}(r)$. It should be mentioned that $\mathcal{V}_{\rm SCF}(r;\omega)$ is a complex function, whereas $\mathcal{V}_{\rm ext}(r;\omega)$ is real.

3 Results and conclusion

In Figs. 2 and 3 the predictions of the total photoionization cross section for Na_{20} as a function of photon energy are presented. The comparison is made between the LDA (independent particle model) and the TDLDA (N-body model) results. The photon impact energy ranges from the $2s$ ionization potential to approximatively 0.5 eV above the $1s$ ionization potential (see Table 1). Figure 2 shows the results from wrong asymptotic conditions, whereas those with the self-interaction correction are reported in Fig. 3. One immediately notes the very important difference existing (notice the logarithm scale on the figures) between the TDLDA cross sections and the LDA ones. As the photon impact energy increases, this discrepancy becomes less and less important. The matrix elements (12) depend upon the real and the imaginary part of the self-consistent field potential $\mathcal{V}_{\rm SCF}(r;\omega)$. We have checked that, in the photon energy range considered here, the real part of the self-consistent field is mostly larger than the external potential. Therefore, the antiscreening (i.e., the fact that the induced potential $V_{\rm ind}(r;\omega)$ in (9) is repulsive) is always dominant, which leads to TDLDA cross sections larger than the LDA ones.

Concerning the independent-particle results, we see that in contrast with the LDA cross section, which vanishes at threshold, we find for the LDA-SIC cross section a finite threshold value. This is a well-known striking feature of final-state interaction effects appearing at low energies [15]. As can be clearly seen from Fig. 3, the opening of $1d$ and $1p$ ionization channels is characterized by a step function in the cross section. Compared to LDA, the SIC leads to many more unoccupied bound states (mainly Rydberg states) since, in this approximation, the effective cluster potential has an asymptotic Coulombic behaviour. Therefore, the final-state level density increases, leading to a more fragmented oscillator strength and, as in the atomic case, the TDLDA-SIC cross section exhibits many sharp one-electron autoionization resonances. These resonances are the consequence of a quantum interference between the direct ionization process and discrete excitations. Since in the LDA, the mixing between different channels is not allowed, either an LDA or LDA-SIC cross section does not display the resonances. Also due to the Coulomb tail $(-1/r)$ of the effective potential, the ejected electron expe-

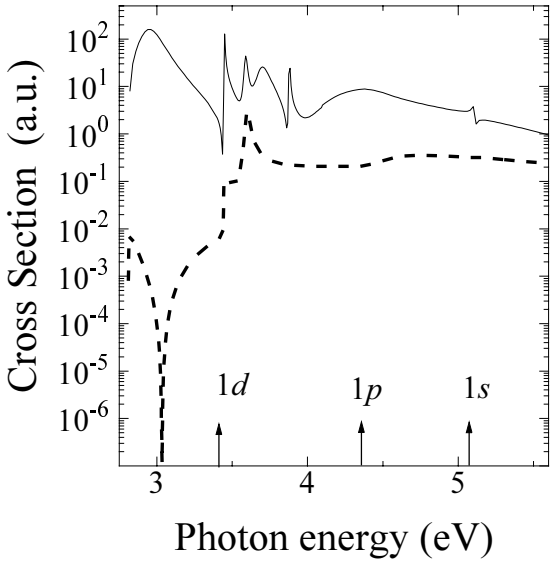

Fig. 2. Total photoionization cross section for Na_{20} as a function of photon energy ω. TDLDA results, full curve; LDA, broken curve. The arrows at the bottom of the figure indicate the ionization thresholds of the occupied orbitals.

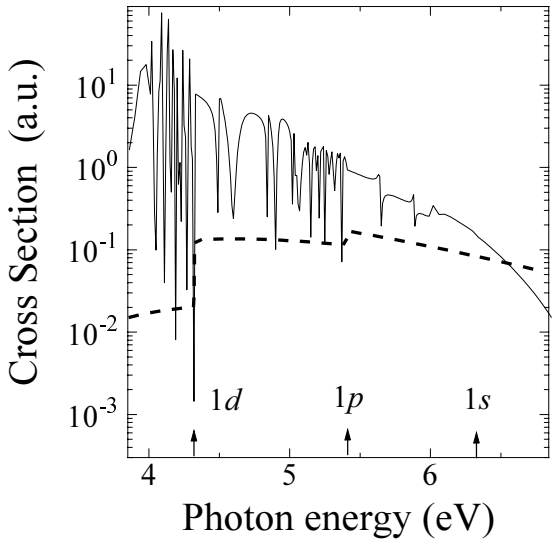

Fig. 3. Total photoionization cross section for Na_{20} as a function of photon energy ω. TDLDA-SIC results, full curve; LDA-SIC, broken curve. The arrows at the bottom of the figure indicate the ionization thresholds of the occupied orbitals.

riences an attractive force and therefore, at a given photon energy, the LDA-SIC and TDLDA-SIC photoionization cross sections are smaller than the LDA and TDLDA ones.

The comparison between the TDLDA and TDLDA-SIC results allows us to conclude that in contrast to the photoexcitation process, the photoionization cross sections are very sensitive to the approximation used to describe the delocalized electrons of the cluster. In order to understand this difference, we propose the following explanations. First, in the TDLDA-SIC photoexcitation cross section (PECS), the largest part of the oscillator strength is situated around 2.5 eV (corresponding to the collective excitation of the surface plasmon), well below the first ionization potential (which is given by the energy of the $2s$ orbital, 3.84 eV (see Table 1)). Thus, the excited states involved in the collective excitation are not localized near the continuum, and therefore the Rydberg states which are specific to the self-interaction correction play a minor role in the photoexcitation process (TDLDA and TDLDA-SIC PECS exhibit similar shapes). Second, since the dramatic changes which appeared in the photoionization cross section are due to an interference process between one bound–continuum transition and one bound–bound transition, it seems very unlikely for one to find two bound–bound transitions with exactly the same energy leading to a dramatic change in the photoexcitation cross section.

It is also interesting to estimate the contribution of the photoionization to the Thomas–Reiche–Kuhn sum rule. In the LDA, the ionization potential (IP) is not simply related to Kohn–Sham eigenvalue of the highest occupied (HO) orbital, but rather is given by the difference between the ground-state energies of the positively charged cluster and the neutral one. Indeed, the $2s$ LDA eigen-energy of Na_{20} (2.81 eV see Table 1) underestimates considerably the experimental IP (3.77 eV) [16]. Furthermore, similarly to Koopman's theorem in HF theory, the energy of the (HO) orbital resulting from "exact" Kohn–Sham calculations is an excellent approximation of the cluster ionization potential. In fact, it is also a good approximation for the approximate LDA-SIC theory, as illustrated by the good agreement between the $2s$ energy (3.84 eV see Table 1) and the experimental IP. This means that, in this approximation, the eigenvalue and eigenfunction associated to the HO orbital can be interpreted as the particle energy and wave function, respectively. It turns out that, in the TDLDA PECS, the oscillator strength is fragmented mainly into two contributions at energies 2.67 eV and 2.96 eV, respectively [11]. Thus, since the energy of the $2s$ orbital is located at an energy smaller than the second maximum of the PECS, a large part (57%) of the sum rule comes from the photoionization process. As already discussed at the beginning of this paragraph, this is not surprising, since standard LDA does not seem to be an adequate theory for the description of the photoionization process. On the contrary, in the TDLDA-SIC PECS, the largest part of the oscillator strength is situated at energies smaller than the energy of the $2s$ orbital, which leads to a contribution of the photoionization to the Thomas–Reiche–Kuhn sum rule of about 9%. Thus, with this correction (SIC), most of the sum rule is contained in the photoexcitation process; this is in agreement with what is known from other works on plasmon response.

Evaluation of photoionization cross sections for other neutral and charged closed-shell alkali-metal clusters is already in progress, and the results will be presented in a forthcoming paper. Finally, we hope that experimenters in the near future will be able to measure photoionization cross sections of simple metal clusters and the associated autoionization resonances that are predicted by the present theory, in order that we may gain a better

understanding of the role played by the many-electron correlations on the photoionization process.

The authors would like to thank the referees for their suggestions for improvement of the manuscript and F. Martín for helpful discussions and comments. We would also like to thank the CNUSC (Centre National Universtaire Sud de Calcul) for providing free computer time.

References

1. W. Ekardt: Phys. Rev. B **31**, 6360 (1985)
2. M. Koskinen, M. Manninen: Phys. Rev. B **54**, 14 796 (1996)
3. O. Frank, J.M. Rost: Z. Phys. D **38**, 59 (1996)
4. A. Zangwill, P. Soven: Phys. Rev. A **21**, 1561 (1980)
5. Z. Levine, P. Soven: Phys. Rev. Lett. **50**, 2074 (1983)
6. M. Stener, P. Decleva: J. Phys. B **30**, 4481 (1997)
7. U. Fano, J.W. Cooper: Phys. Rev. **137**, A1364 (1965)
8. See, for instance, M. Brack: Rev. Mod. Phys. **65**, 677 (1993) and references therein
9. O. Gunnarsson, B.I. Lundqvist: Phys. Rev. B **13**, 4274 (1976)
10. M. Madjet, C. Guet, W.R. Johnson: Phys. Rev. A **51**, 1327 (1995)
11. J.M. Pacheco, W. Ekardt: Ann. Phys. **1**, 254 (1992)
12. J.M. Pacheco, W. Ekardt: Z. Phys. D **24**, 65 (1992)
13. P. Stampfli, K.H. Bennemann: Phys. Rev. A **39**, 1007 (1989)
14. J.P. Perdew, A. Zunger: Phys. Rev. B **237**, 5048 (1981)
15. C.J. Joachain: *Quantum Collision Theory* (North-Holland, Amsterdam 1975)
16. M.M. Kappes, M. Schär, U. Röthlisberger, G. Yeretzian, E. Schumacher: Chem. Phys. Lett. **143**, 251 (1988)